Diyala Journal of Engineering Sciences

Journal homepage: https://djes.info/index.php/djes

ISSN: 1999-8716 (Print); 2616-6909 (Online)

Numerical Analysis of Reinforced Concrete Exterior Beam-Column Joints Under Limited Cycles of Repeated Loading

Hadeel Ali Handel Sabah*, Ibrahim S. I. Harba

Department of Civil Engineering, University of Nahrain, Baghdad, Iraq

ARTICLE INFO

Article history:
Received October 2, 2022
Accepted November 8, 2022

Keywords:
Beam-column joint
Numerical model
Limited cycles of repeated loading
Concrete damage plasticity model

ABSTRACT

The beam-column joints play an important role in the structures where the functions of connection shortage by transport the forces like shear, moment, and torsion from the beam to the column. So, this study represents an attempt to investigate the performance and the effect of limited cycles of repeated load on the strength of the exterior beam-column joint core. Therefore, 34 specimens have been investigated by using a numerical analysis that used the finite element method. To simulate these specimens, the concrete damage plasticity model was used to define the concrete materials and the nonlinear isotropic/kinematic (combined) hardening model for steel material definition. These models are involved in the ABAQUS software package, version 2020. This study involves key parametric studies on beam-column joints, which are summarized as changing the ratio of shear reinforcement of the joint core in addition to using two types of shear reinforcement. This study also includes the effect of flexural reinforcement of the beam as well as the beam's shear reinforcement effect on the strength of the beam-column joint. To calibrate the software to simulate a realistic result, three specimens have been used, which have been tested in previous studies. It has been found that this numerical model accurately predicts the experimental response under limited cycles of repeated loading. The ultimate load from modelling was compared with the experiment once, having a difference of less than 10% and the ultimate displacement having a difference of less than 11%. It has been found that increasing the ratio of the joint's shear reinforcement to double has no significant effect on the ultimate load. Otherwise, decreasing it to half leads to a decrease in the ultimate load compared with a specimen that is designed according to ASCE352-02R. This study has studied the effectiveness of increasing the shear reinforcement by adding an x-shape reinforcement. Also, the flexural reinforcement of the beam has found it has increased the ultimate load capacity by 48% Where the ratio of flexural reinforcement increased to 1.8%, the load bearing capacity was enhanced.

1. Introduction

The behavior of beam-column connections has long been identified as a critical part that usually plays a significant role in the overall behavior of Reinforced Concrete framed structures subjected to seismic loading. Even when considered separately, complicated interacting variables like shear, bond, confinement, and fatigue have an impact on how RC connections respond [1].

During earthquake the structure expose to repetitive application of a load (fluctuating stresses, forces, strains, forces, etc.) on a structural element degrades the material and eventually results in fatigue, these loads could be simulated as cycles loading. Cycles loading

* Corresponding author.
E-mail address: hadeelhandel8@gmail.com
DOI: 10.24237/djes.2022.15410

divided to three types reversed, repeated, and fluctuating cyclic loading as shown in Figure 1.

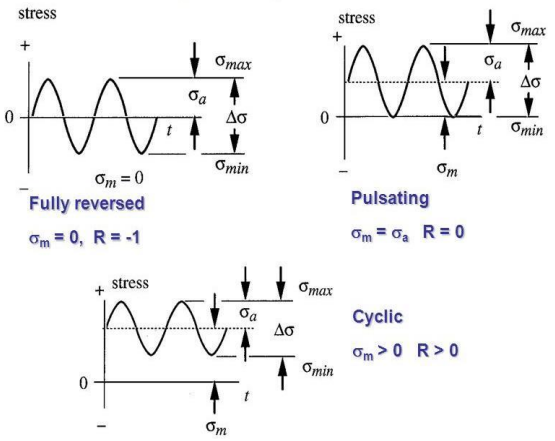

Figure1. Types of cyclic loading

A joint's focus is to help its adjacent members to ultimate capacity sustain. Three different types of joints corner, exterior, and interior joints can be found in a moment-resisting frame. When an earthquake occurs, the external joint's behavior of the beam-column junction responds more negatively than the interior joint due to effect of the moment and shear capacity as a result of unbalanced structures of beam-column joint frame. Joint failure may result from shear failure, anchorage failure, or a combination of the two.

Favvata, et al. [2] established an effective and efficient model to investigate the impact of the local nonlinear response of RC exterior beam-column joints on the parameters' ductility of columns, failure mode, and overall seismic response of a multistory RC frame structure. A model was created by using advanced software for nonlinear static and dynamic analysis ADAPTIC. This study showed that the multistory frame failure mode significantly differs from that when beam-column joints are viewed as rigid because plastic hinges do not appear in the beams next to the connections; the damage of the region of the joints' core leads in a reduction in the columns' maximum ductility requirements at the multi-story structure base; and when compared to rigid joint modelling, the 8-storey frame structure's maximum inter storey drifts often increase.

Saito and Kikuchi, [3] created a new large-deformation model of the beam-column connection and non-linear behaviour of reinforced concrete frames under limited cycles of repeated loading. The present model is made up of a reinforcing elements and multi-node joint panel zone. By utilizing the modified compression field theory (MCFT) developed by Vecchio etal. [4], the model takes into account the bond-slip of the reinforcing and the beam-column junction's shear behaviours. The results of this investigation point to the pinching effect and energy dissipation caused by bond-slip and joint shear behavior in the beam-column junction. The absorption of hysteretic energy is considerably overestimated if the shear deformation of the joint and bond-slip are not taken into account.

Diro and Kabeta, [5] investigate a nonlinear finite element model by using ABAQUS software to identify the joint shear mode of failure in terms of joint shear capacity, deformation, and cracking pattern for a reinforced concrete exterior beam-column joint exposed to lateral stress. The enhancement in the beam's ratio of the longitudinal tension reinforcement did not reveal any significant change in shear strength with the addition of a small quantity of tensile reinforcement. On the other hand, the cracking pattern may significantly change from the edge of the beam to the edge of the column. Additionally, it shows a higher shear resistance capacity during the concrete crushing stage.

Cao, et al., [6] estimated the moment in the beam-column joint by using experimental result data. Researchers investigated the potential for high nonlinearity in the proposed beam-column connection in concrete frames. The Extreme Learning Machine demonstrates its value as a static tool by producing results that are similar to those of the experimental one while estimating the moment of the concrete beam-column joint.

AL-Jmailyand and Rahman, [7] developed a model by ABAQUS software, to simulate a possible model of beam-column junction in any typical structure facing reversed-cyclic load from earthquakes. The proposed model provides a clear illustration of the plastic mechanisms

that define joint behaviour when subjected to repeated seismic actions' shear loading. The objective of this research is to identify the energy and residual shear strength that the joint maintains until it reaches the yield point during such reversible cycles. To determine the overall deformation after the cycles and to understand the response of that joint after each cycle and at the end, shear capacity and column deformations are computed after each applied cycle, obtained from the earthquake and accumulation. After a few cycles, the section was yielding and gaining more energy, causing larger load deformation relation cycles until the concrete's crushing (compressive stress) achieved its maximum and the entire section collapsed. Since reinforcements cannot be seen, it is suggested that the cracks in old buildings be carefully marked and investigated after each earthquake to determine whether there is progress in spreading.

This study is more comprehensive than previous studies in that it investigates the effect of combined shear reinforcement, in addition to shear and flexural reinforcements of the beam, on the joint core behaviour and load capacity.].

1.1 Objectives of the study

The objective of this study summarized by; investigation the two key parameters' effects on the shear strength of reinforced concrete exterior joints: joint aspect ratio of shear reinforcement; and joint shear demand by control on the ratio of beam longitudinal reinforcement. In addition to investigate the influence of shear deformation of RC exterior beam-column joint under limited cycles of repeated loading. Finally, developments of suitable efficient schemes for beam-column joints of cyclic loading designed structures to achieve the modern ductile structure deigning.

2. Methodology

The present work studies the key parameters that effect the strength of the beam-column joint under limited cycles of repeated loading by using ABAQUS software 2020, which including the effect of shear reinforcement, using different shapes of shear reinforcement, in addition to effect of flexural reinforcement.

2.1 Validation work

The validation is containing three models that will be respect to experimental work of Chalioris etal. [8], which designed according to ACI-318 code with different joint core reinforcement as shown in Figure 2, so there are three main parts (concrete body, reinforcement steel (main reinforcement of beam and column, ties of column and stirrups of beam, X-bar and loading plates) and their details are shown in table1 and Figure 2.

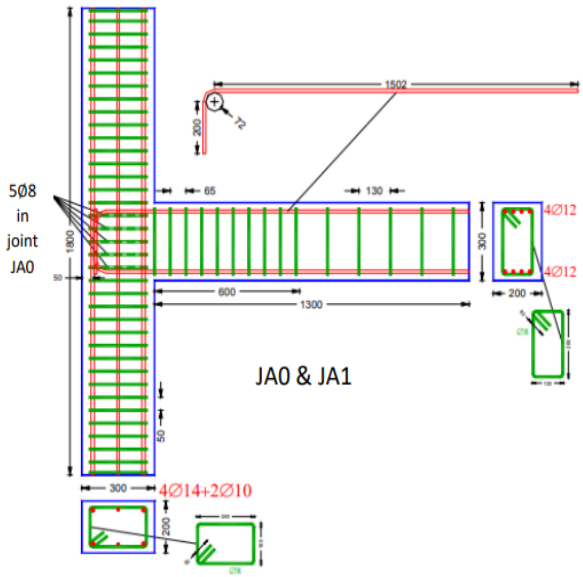

Figure2. Experimental model detailing [7]

2.2 Constitutive model of concrete

Concrete has been considered to be linear elastic at stress levels up to 30% of its compressive strength. Modulus of elasticity, Ec has been calculated according to E=4700$\sqrt{f_c'}$. Poisson ratio, ν, of 0.2 has been adopted. Solid 8-node brick element with reduced integration (C3D8R) has been used to simulate the concrete. The plastic behaviour has been defined using concrete damage plasticity model (CDP) with the default parameters that proposed by ABAQUS which are summarized in Table 1.

Table 1: Summarized the details of validation models (Chalioris etal. 2007)

Material \ Element		Beam	Column	Joint core	Mechanical properties	
Concrete properties	Cross section	200*300 (mm)	300*200 (mm)	200*200 (mm)	f_c'	34 MPa
					E	28600MPa
					v	0.2
Steel properties	JA0	2(4Ø12) Ø8@65mm	4Ø14+2Ø10 Ø8@50mm	Ø8@50 mm	f_y	580 MPa
	JA1	2(4Ø12) Ø8@65mm	4Ø14+2Ø10 Ø8@50mm	Nil	E	205000MPa
	JC9	2(4Ø12) Ø8@65mm	4Ø14+2Ø10 Ø8@50mm	2X-Ø12	v	0.3

JA0 is the control sample (sample which designed according ACI 318-19 recommendations)
JA1 is the sample has no reinforcement at joint region
JC9 is the sample which has X-bar as shear joint reinforcement

Uniaxial stress-strain behaviour of concrete is simulated utilizing Saenz [9], model as shown in Figure 3.

Concrete in tension has a two-part uniaxial stress-strain behaviour. The first section has a linear elastic behaviour up to the concrete tensile strength, as illustrated in Figure 4.

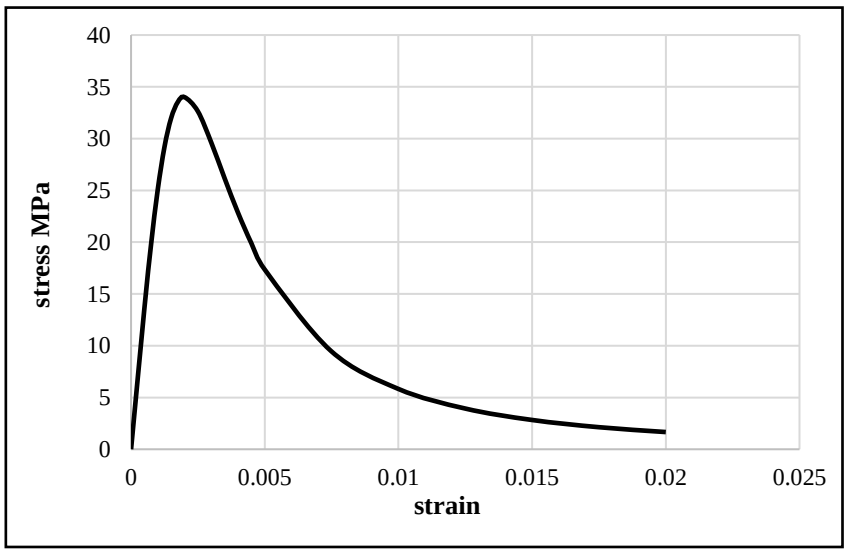

Figure 3. Compressive stress-strain curve [8]

The start of the second phase corresponds with the occurrence and propagation of cracks in concrete under tension, which is illustrated by a descending branch in the diagram of uniaxial tensile stress-strain curve. According to Belarbi and Thomas [12], the behaviour during this

phase is represented using a softening technique that might use linear, bilinear, or nonlinear stress-strain relationships.

The linear behaviour is used to the model in this study in accordance with the analytical assumptions. Details of the tensile softening assumptions used in the given model are shown in Figure 4.

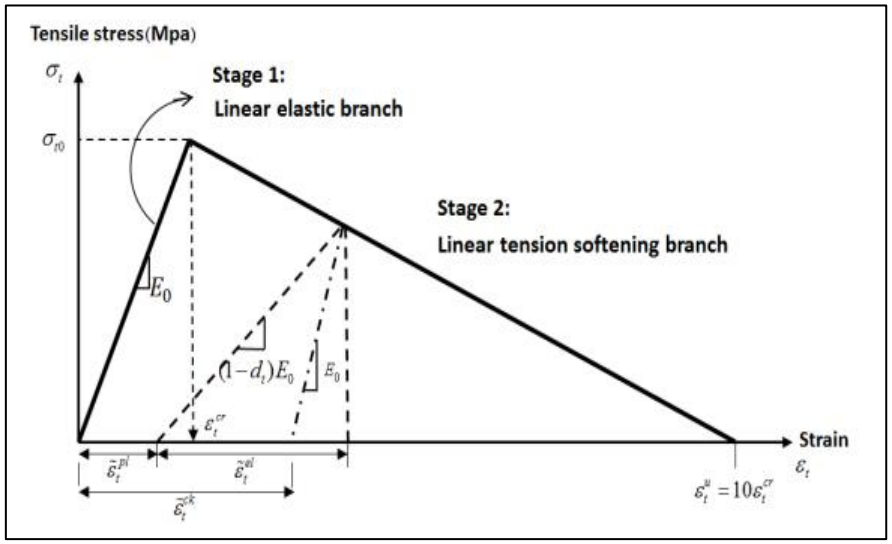

Figure 4. Concrete uniaxial tensile stress-strain behaviour and its softening branch assumptions

To calculate the ultimate tensile strength of concrete, using Eq. (Wang and Vecchio; Genikomsou and Polak) [10,11].

$\sigma_t = E_c \varepsilon_t$ if $\varepsilon_t \leq \varepsilon_{cr}$ (1)

$\sigma_t = f_t(\frac{\varepsilon_{cr}}{\varepsilon_t})^n$ if $\varepsilon_t > \varepsilon_{cr}$ (2)

$\acute{f}_t$=0.33$\sqrt{\acute{f}_c}$ (MPa) (3)

where ε_{cr} is the cracking strain which assumed to be equal 0.00012; σ_t *and* ε_t are the tensile stress and strain; respectively.

The concrete damage plasticity model defines damage in terms of both uniaxial tension and compression throughout the softening process. As soon as the maximum uniaxial compressive strength, or strain level ε_0, is reached, damage in compression starts to happen. Two damage factors, d_t and d_c, which stand for tensile and compressive damage, respectively, and are thought to be components of the plastic strains, describe how elastic stiffness decreases in the softening regime. The concrete damage plasticity model in the given numerical model assumes that tensile and compressive damage occur in accordance with the following equations and diagrams of Figure 5.

$d_t = 1 - \frac{\sigma_t}{E_o(\varepsilon_t - \varepsilon_t^{pl})}$ (4)

$d_c = 1 - \frac{\sigma_c}{E_o(\varepsilon_c - \varepsilon_c^{pl})}$ (5)

where σ_t and σ_c are the tension and compression stresses; respectively. ε_t and $\varepsilon_c$are the tension and compression strains; respectively. $\varepsilon_t^{pl}$and ε_c^{pl} are the plastic tension and compression strains. Therefore, the tension stress-displacement curve could be drawn as shown in Figure 6

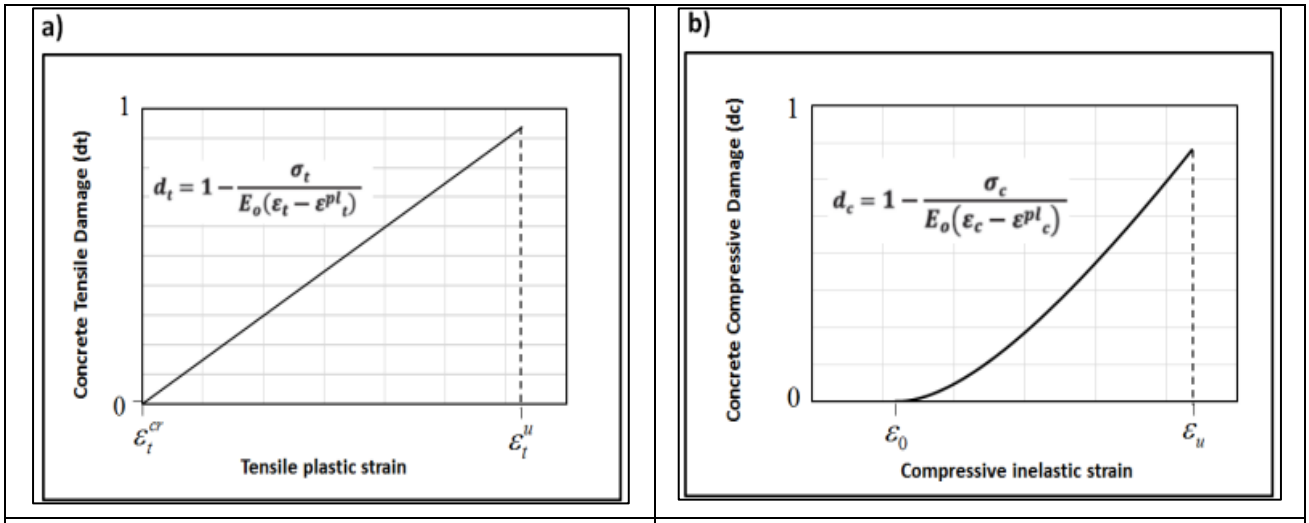

a) b)

Figure 5. Definition of damage parameter in CDP model: a) Uniaxial tensile damage; b) Uniaxial compressive damage

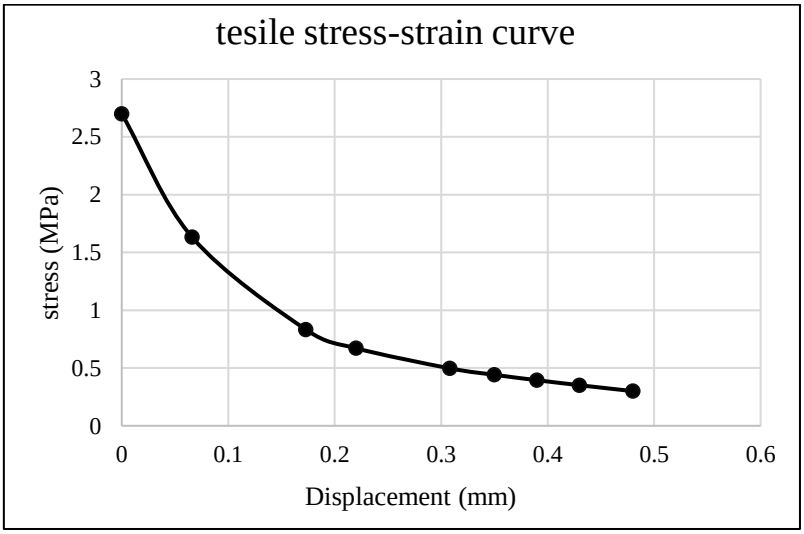

Figure 6. Input tensile stress-displacement curve in Abacus software

2.3 Constitutive model of steel

The stress-strain curve behaviour when applied limited cycles of repeated loading must be determined since the steel reinforcement has a ductile characteristic (large inelastic strains). However, under static loading, the behaviour of the uniaxial stress-strain curve is elastic-perfect plastic. But according to SIMULIA/ABAQUS (2016), for metals subjected to limited cycles of repeated loading. A linear kinematic hardening model or isotropic/kinematic hardening model should be used. According to Figure 7, isotropic hardening refers to the yield surface changing size evenly in all directions, causing the yield stress to rise (or fall) in every stress direction while plastic straining occurs.

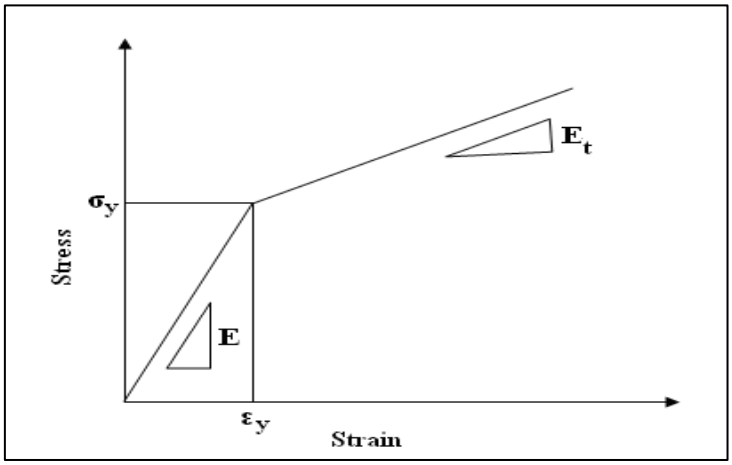

Figure 7. The isotropic hardening stress-stain curve for biaxial material [12]

According to von Mises theory, the stress is changed by increasing the strain under static loading, as illustrated in figure 8a. But for limited cycles of repeated loading, this behaviour will not be convenient because the difference in stress at the same cycle of loading is constant, as shown in figure 8b. Although the kinematic model gives the behaviour under cyclic load, it does not involve the behaviour of the softening part, which is important to simulate the real behavior of steel material. So, ABAQUS software has combined the isotropic and kinematic hardening models by selecting the hardening combined option. This option requires engineering stress-true plastic strain curve. After determining the best model of software, the stress-strain curve could be obtained by using the proposed formula by Belarbi [12].

Suggested a simplified bilinear constitutive model of concrete and steel bars that are embedded in it (Figure 9). The first has a slope that represents the elasticity modulus of the steel, which is E_s, which covers the elastic range of stresses, and the second has a slope that represents the plastic range shape of which is E_P^*.

However, most models of the materials that display ductile behaviour (large inelastic strains) yield at stress levels orders of magnitude below the material's elastic modulus, suggesting that the important stress and strain indicators are "true" stress (Cauchy stress) and logarithmic strain. If nominal stress-strain data of an isotropic material for a uniaxial test were presented, it would be easy to convert to true stress and logarithmic plastic strain, as shown in eq.2 and eq.3 (Yang, 2018).

$$\sigma_{true} = \sigma_{nom}(1 + \varepsilon_{nom}) \quad (6)$$

$$\varepsilon^{pl} = \ln(1 + \varepsilon_{nom}) - \frac{\sigma_{true}}{E} \quad (7)$$

Therefore, the models' data for the material should be provided in these measurements. Finally, the input data could be obtained, and the stress-strain has been obtained as shown in Figure10.

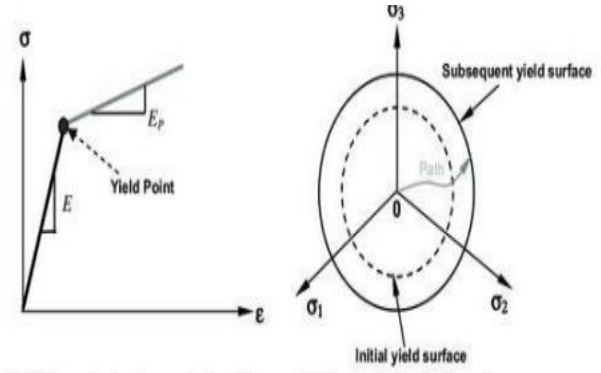

a)

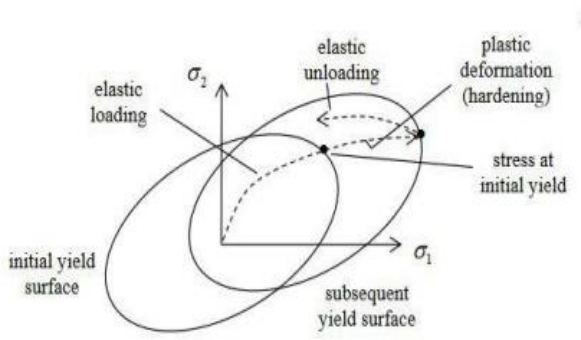

b)

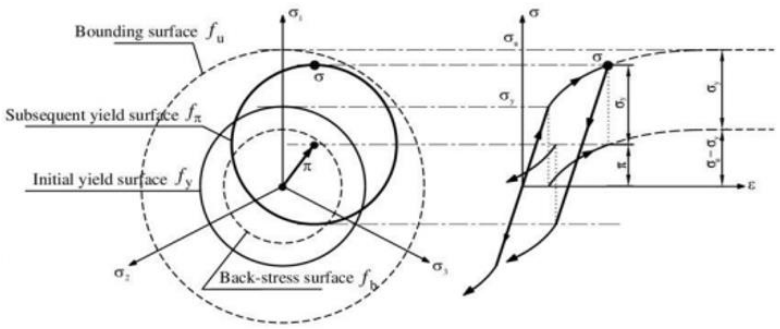

c)

Figure 8. Representation of yield surface and stress-strain curve for different material; (a) isotropic hardening (b) kinematic hardening (c) combined hardening [13]

2.4 Loads and boundary condition

There are two types of loads: static and cyclic, so the model should have two steps; the axial load applied according eq. Nc=0.05$Agf\acute{}\ c$ which is applied at the first step (initial).

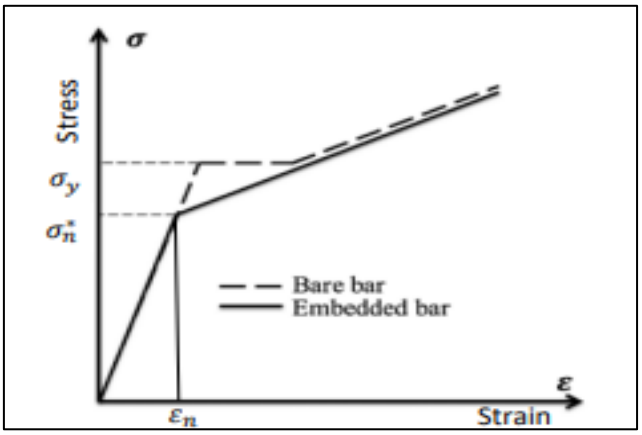

Figure 9. Stress-strain relation for steel reinforcement [14]

The limited cycles of repeated loading are imposed by using the time history of Chalioris etal. [8] as shown in figure11. The second step's application of the amplitude function was utilized to simulate the static situation in the implicit solver. And it has been used in analyses where the main goal is a final static response by employing quasi-static applications, which include inertia effects mainly to regularize unstable behaviour. In order to reduce large time increments are taken wherever possible.

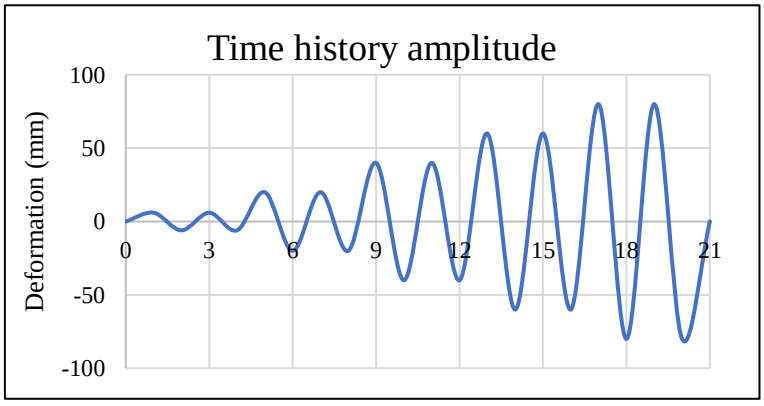

Figure 11. Amplitude limited cycles of repeated loading [7]

Considerable numerical dissipation may also be employed to achieve convergence at specific points in the loading history, as shown in figure12B, which also shows how the loads are defined. The boundary conditions at each simulation are a fixed end column and a roller restriction on the other end (free motion at static load applied). As illustrated in figure 12A, these constraints were applied using hinged supports with all transitional degrees of freedom in the global X, Y, and Z directions restricted, and roller supports with restricted transitional degrees of freedom in the global X and Z directions. After parts are assembled, the associated interaction between them must be defined. The perfect bond between the concrete surface and the corresponding load plates' surfaces by choosing the tie constraint, although this is not the actual assumption, reduces the time as the bond isn't involved in the parametric study. The same assumption is made for the concrete and embedded parts by using the embedded region constraint. In addition, to make the result more easily extractable, the beam's plates could be combined by using an equation constraint option as shown in Figure 13.

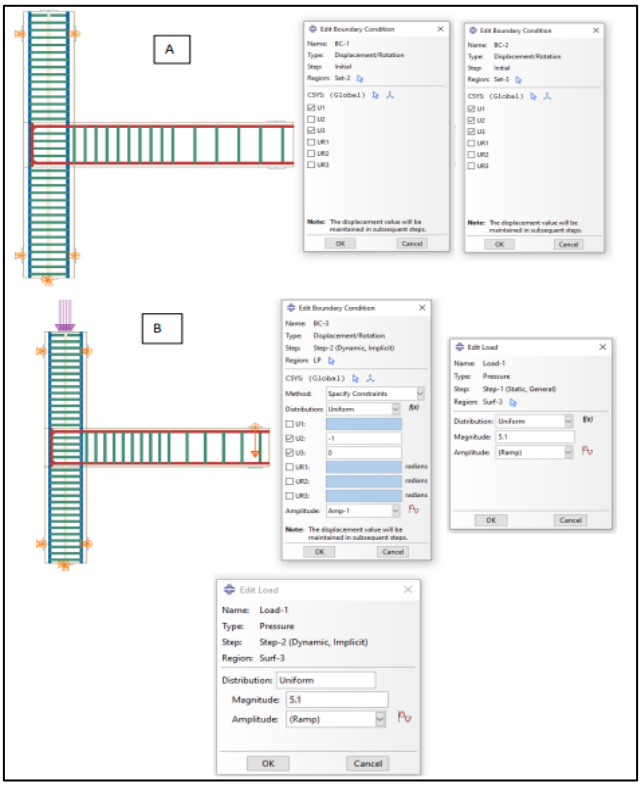

Figure 12. A) The boundary condition definition; B) Loads definition

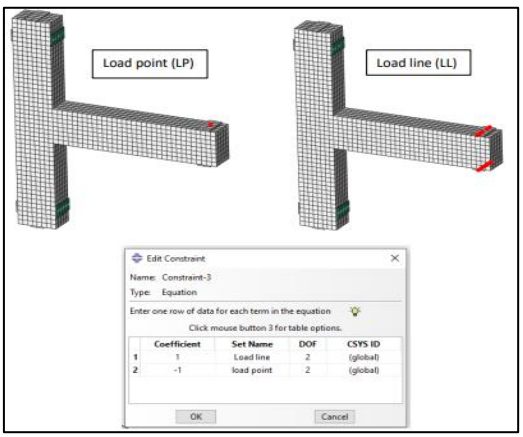

Figure 13. Embedded equation of LL. And LP

2.5 Meshing and convergence study

Convergence in finite element analysis (FEA) refers to the partial differential equations' (PDEs') true solution being achieved as that of the geometry, or spatial domain, is meshes more finely. Reducing the size of the element and evaluating how this affects the solution's accuracy are both parts of the mesh convergence process.

As the design's behaviour or model is better sampled over its physical domain, the smaller size of the mesh generally provides a more accurate result. In this study, the convergence will be studied for three mesh sizes: 20, 40, and 60. So, the hysteric curve is wider for the numerical simulation than the experimental. And as size is reduced, an accurate convergence is obtained as well as the ultimate and failure point being closer. Therefore, the size 20 mesh gives the best result, but it takes more time to run. So, as compared, the differences between 20, 40, and 60 mesh are 2.12%, 0.71%, and 3.96 for load, 1.69%, 3.17%, and 3.46% for displacement, respectively. That result shows that the mesh 40 is the best choice, as shown in Figure 14.

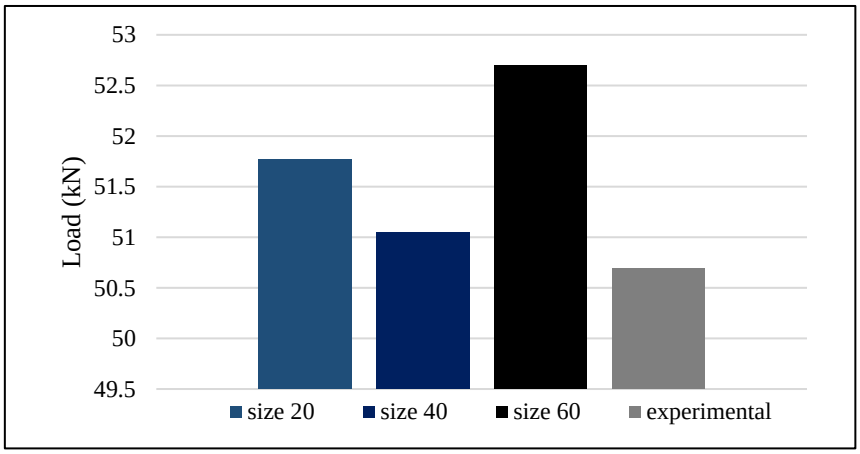

a)

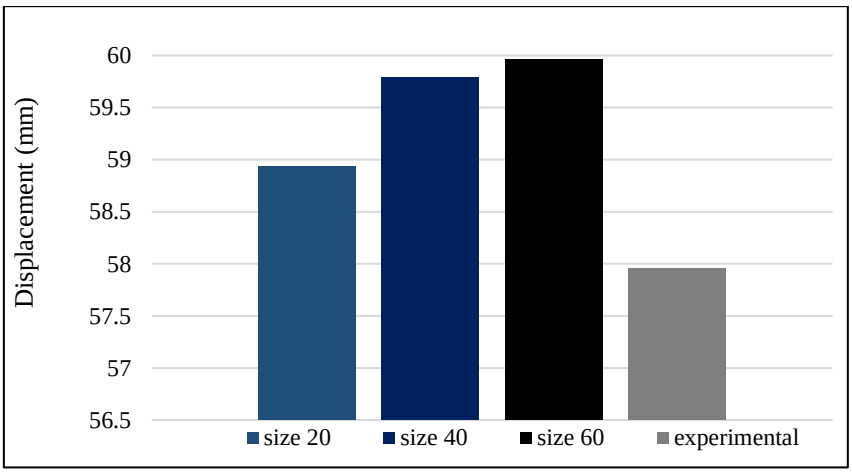

b)

Figure 14. Comparison of convergence study

Figure 15 shows the validation of the failure shape of the JA0 sample by using 40 mesh, where it is almost similar for both experimental and numerical results.

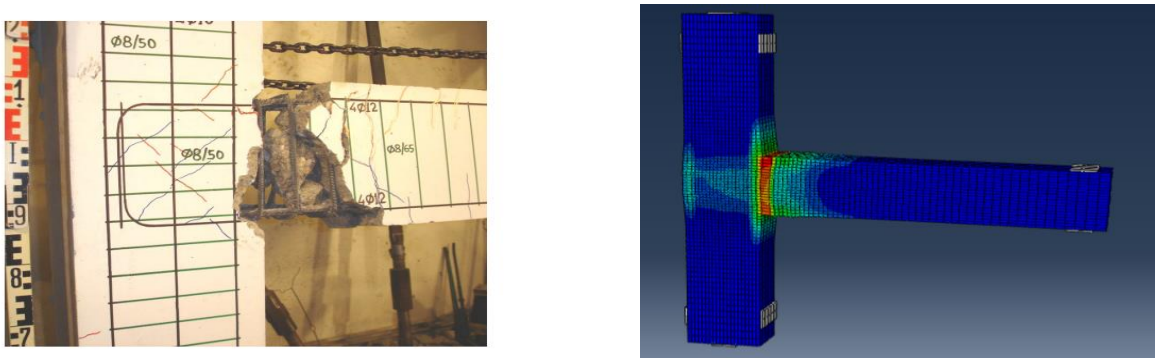

a) b)

Figure 15. Failure in joint of external beam-column joint (a) Experimental test [7]; (b) Numerical model

2.6 Parametric study

The parametric study for this study has been divided into 8 groups. They include the most key parameters that might have an effect on the behaviour of the joint. The first parameter is the effect of shear reinforcement of the joint core when using different reinforcement types as shown in figure 16. The second parameter is the effect of shear reinforcement of the beam by investigating the spacing and ratio of shear reinforcement. The last one is by investigating the ratio of main reinforcement of the beam. These parameters are summarized in Table 2.

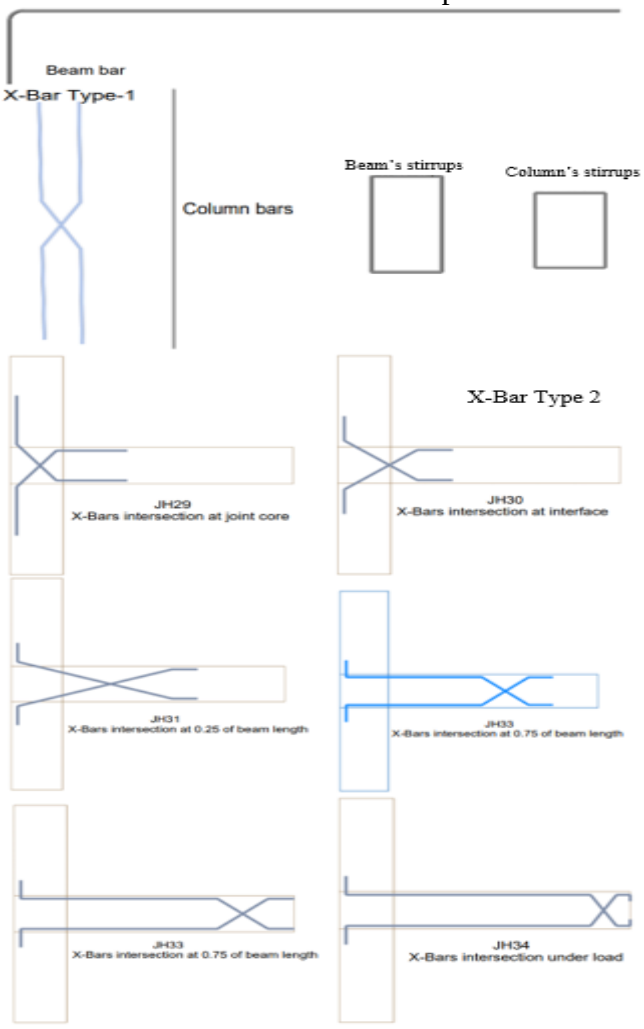

Figure 16. The reinforcement types of beam and column

Table 2: summarized the parametric study

Group NO.	Specimen's ID	Joint reinforcement				Beam reinforcement	
		Ties	ρ_{ties}%	X-bars	ρ_{Xbars}%	Stirrups	Top & bottom reinforcement
A	JA0*	5Ø8	0.838	N/A	N/A	Ø8@65mm	4Ø12
	JA1	N/A	0				
	JA2	3Ø8	0.503	N/A	N/A	Ø8@65mm	2(4Ø12)
	JA3	5Ø12	1.885				
B	JB4					Ø8@35mm	
	JB5	N/A	N/A	N/A	N/A	Ø8@50mm	2(4Ø12)
	JB6					Ø8@70mm	
	JB7					Ø8@85mm	
C	JC8			1-Xbar Ø12	0.589		
	JC9	N/A	N/A	2-Xbar Ø12	1.178	Ø8@65mm	2(4Ø12)
	JC10			1-Xbar Ø16	1.0472		
	JC11			2-Xbar Ø16	2.094		
D	JD12	3Ø8	0.503	2-Xbar Ø12	0.589	Ø8@65mm	2(4Ø12)
	JD13	5Ø12	1.885	1-XbarØ16	1.0472		
	JD14	3Ø8	0.503	2-XbarØ12	1.178	Ø8@70mm	
	JD15	5Ø12	1.885	1-XbarØ16	1.0472		
	JD16	3Ø8	0.503	2-XbarØ12	1.178	Ø8@50mm	
	JD17	5Ø12	1.885	1-XbarØ16	1.0472		
E	JE18	5Ø8	0.837			Ø12	
	JE19	5Ø8	0.837	N/A	N/A	Ø10	2(4Ø12)
	JE20	5Ø8	0.837			Ø6	
	JE21	5Ø8	0.837			Ø4	
F	JF22	N/A	N/A	2X-barØ12	1.178	Ø12	2(4Ø12)
	JF23	N/A	N/A	2X-barØ12	1.178	Ø10	
	JF24	N/A	N/A	2X-barØ12	1.178	Ø6	
	JF25	N/A	N/A	2X-barØ12	1.178	Ø4	
G	JG26						2(4Ø16)
	JG27	5Ø8	0.837	N/A	N/A	Ø8@65	2(4Ø18)
	JG28						2(4Ø20)
H	JH29						
	JH30						
	JH31	N/A	N/A	2X-barØ12	1.78	Ø8@65	2(4Ø12)
	JH32						
	JH33						
	JH34						

3. Results and discussion

The RC beam-column connections' results are displayed as force and displacement bar charts, ultimate loads and displacements curves, and cracking patterns that are observed at several key points of the connection joints' shear behaviour.

3.1 Validation of numerical modelling

Performing the validation is essential to ensure the property of the damage plasticity model as well as the compatibility of the experimental work with software model. The validation model, which was designed according to ACI-352R-02 (JA0), gave almost an ideal validation for both displacement and load. Also, the models of (JA1 &JC9) were given an acceptable result. The experimental load and displacement values were from Chariols et al. [8] and compared with numerical results from ABAQUS software 2021. Figure17 shows the difference between the numerical and experimental results. They also have different

validation curve shapes as well as the values between experimental and abaqus results, especially for joints without reinforcement as shown in table 3. Figure 17 show the difference between the numerical and experimental results. Different validation curves were determined as well as the values between experimental and Abaqus software results, especially for joints without reinforcement, as shown in Table 3. Because Abaqus software employs a finite element method, which is numerical and does not simulate all of the environments that surround the specimen, as well as using approximate models to simulate the materials and condition of the member during conditions such as cracks and so on, exact values may not be obtained. But they may be close. As well as, the hysteric load of samples showed that the numerical response was wider and larger than experimental one. However, both responses stayed closer at ultimate point, as illustrated in Figure 17. That conclusion could be checked when comparing the numerical specimens of JA0, JA1, and JC9 results (Figure 17D). JA0 had the higher strength more than JA1 and JC9. JC9 improved the strength compared with JA1, which is the same result for the experimental sample (Chariols et al., [8]). These results help to make a close view of the reality for all other parametric studies. Then, the results were compared with numerical JA0, which was the control specimen, as shown in Table 4.

Table 3: Error percentage for load and displacement of validation models

	EX. Load (kN)	Numerical load (kN)	Error%	EX. Disp. (mm)	Numerical disp. (mm)	Error%
JA0	51.36	55.559	7.6%	39.80	42.459	6.3%
JA1	53.70	58.78	9.5%	34.73	39	11%
JC9	53.50	54.011	0.9%	34.94	38.658	9.6%

3.2 Numerical results

This chapter study the observe the result of most common parametric that could effect on the strength of beam column joint, and at this section could summarize these result as well as their difference respect to JA0 at follow table4:

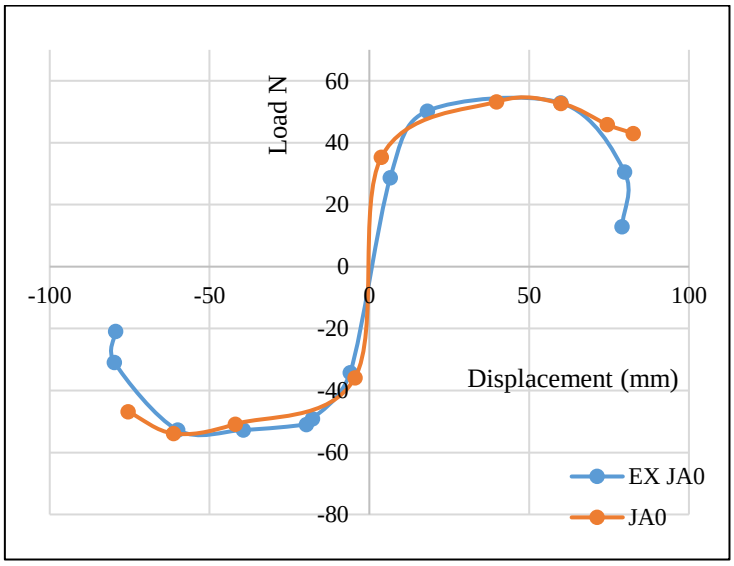

a)

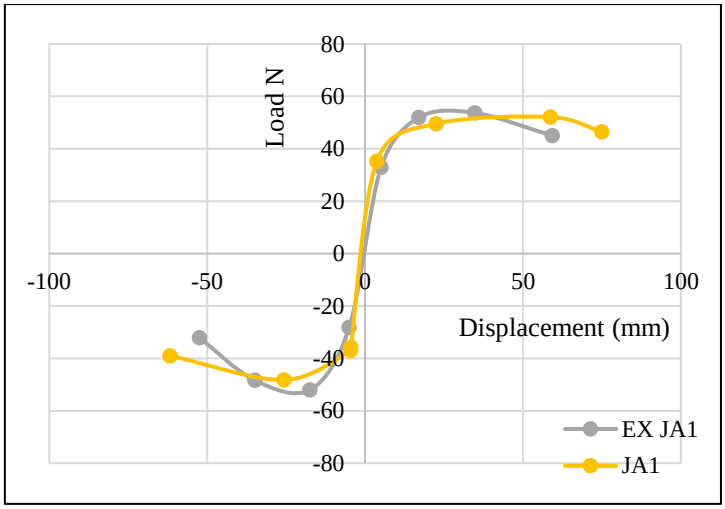

b)

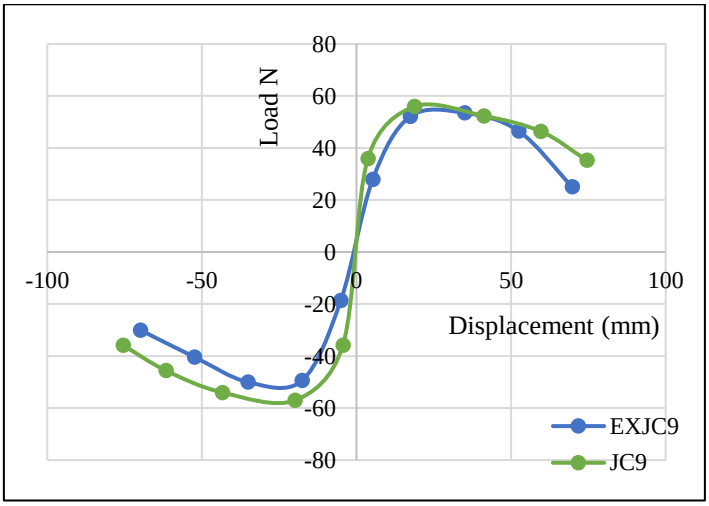

c)

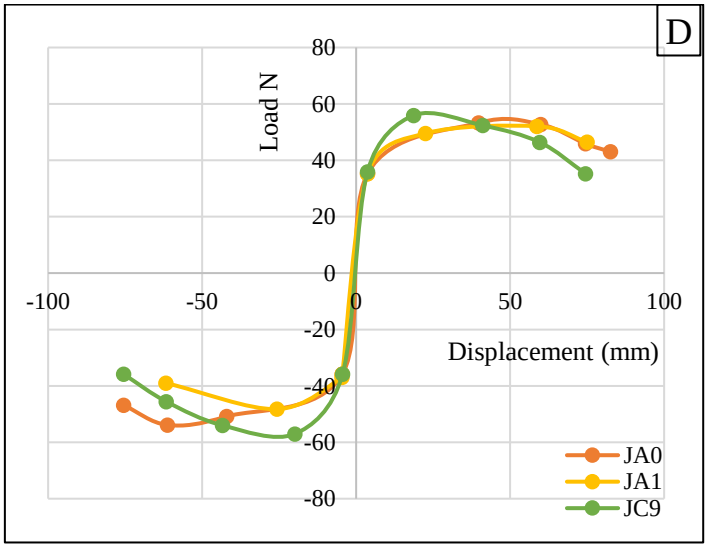

d)

Figure 17. The envelope curve for the experimental and numerical result of three models

3.2.1 Effect of joint's shear reinforcement ratio

The group A study the effect of shear reinforcement at joint core. As illustrate in table 4, the result of the inadequate reinforcement (JA2) was decreased by 3.65% than the control specimen (JA0) for ultimate displacement with dramatic load carrying capacity decreasing, and the specimen with additional reinforcement ratio had more strength than JA2, but at the same load of JA0, it gives more displacement by 4.18%. The doubling of the reinforcement ratio has less effect as compared to 0.84%. This effect on the strength of beam-column joint is due to concrete crushing, which occurs before the steel reinforcement reach yield strength.

Table 4: Summarized the result of parametric study

Group NO.	Joint Name	NO. cycle	NO. cycle at ultimate load	Ultimate load (kN)	Difference	Ultimate displacement(mm)	Difference
A	JA0	10	6	55.559		42.459	
	JA1	10	5	36.6926	-33.96%	40.909	-3.65%
	JA2	10	7	53.6209	-3.49%	40.683	-4.18%
	JA3	10	6	55.494	-0.12%	43.121	1.56%
B	JB4	10	6	42.868	-22.84%	40.230	-5.25%
	JB5	10	6	42.208	-24.03%	40.500	-4.61%
	JB6	10	6	42.5039	-23.50%	41.056	-3.30%
	JB7	10	6	42.206	-24.03%	42.322	-0.32%
C	JC8	10	6	54.953	-1.09%	42.602	0.34%
	JC9	10	6	54.011	-2.79%	42.817	0.84%
	JC10	10	6	54.1176	-2.59%	42.172	-0.68%
	JC11	10	6	53.7949	-3.18%	42.159	-0.71%
D	JD12	10	6	54.723	-1.50%	43.402	2.22%
	JD13	10	6	53.758	-3.24%	41.802	-1.55%
	JD14	10	6	54.5436	-1.83%	43.414	2.25%
	JD15	10	6	53.628	-3.48%	43.399	2.21%
	JD16	10	6	54.8886	-1.21%	43.409	2.24%
	JD17	10	6	53.7581	-3.24%	43.411	2.24%
E	JE18	10	6	55.57	0.02%	43.360	2.12%
	JE19	10	6	55.536	-0.04%	43.410	2.24%
	JE20	10	6	55.443	-0.21%	43.155	1.64%
	JE21	10	6	55.5217	-0.07%	43.300	1.98%
F	JF22	10	6	54.081	-2.66%	42.945	1.14%
	JF23	10	6	54.237	-2.38%	41.237	-2.88%
	JF24	10	6	53.967	-2.87%	42.743	0.67%
	JF25	10	6	53.026	-4.56%	42.977	1.22%
G	JG26	10	10	82.719	48.88%	60.889	43.41%
	JG27	10	10	100.989	81.77%	74.783	76.13%
	JG28	10	10	102.143	83.85%	76.284	79.66%
H	JH29	10	9	75.795	36.42%	57.387	35.16%
	JH30	10	9	63.274	13.89%	74.911	76.43%
	JH31	10	2	36.81	-33.75%	4.450	-89.52%
	JH32	10	2	42.61	-23.31%	5.460	-87.14%
	JH33	10	2	36	-35.20%	3.960	-90.67%
	JH34	10	10	36.046	-35.12%	4.157	-90.21%

3.2.2 The influence of beam's stirrups

This section includes specimens of group B that involved changing of beam's stirrups spacing. The displacement increased as the stirrups' spacing of beams increased, while a small difference in the ultimate load noticed. The ratio of displacement as compared with JA1 was between -1.66% and +3.46% as shown in Figure 18.

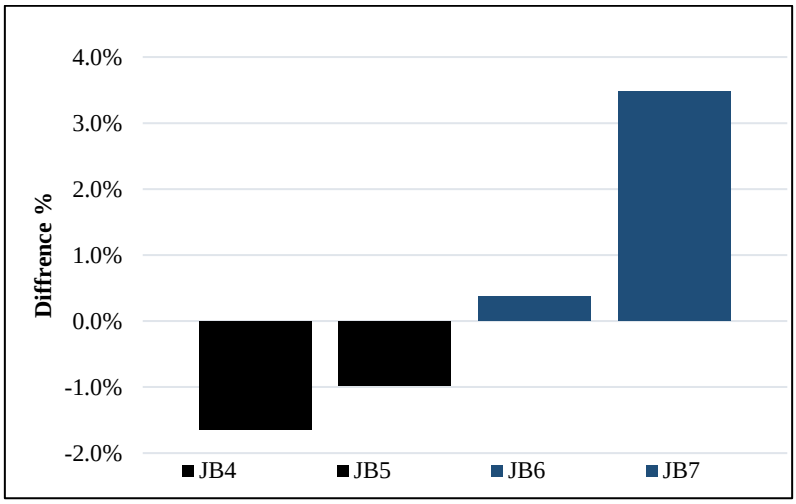

Figure 18. Percentage of displacement ratio of each group B specimen to JA1

3.2.3 Using X-bar reinforcement (Type1)

This section presents the results of group C which involve four RC external beam-column joint specimens in an effort to determine how well crossed inclined bars behave as shear reinforcement in the joint area. Based on the bar chart of hysteretic responses, which shown in figure 19, and cracking modes of the tested joints, it can be concluded that the joints with X-bar reinforcement performed much better overall than the response of the specimen without stirrups. Joints with X-bars demonstrated greater load capacities in the majority of the loading cycles and enhanced hysteretic energy dissipation almost throughout the entire loading sequence when compared to the control specimen without stirrups. This improvement was more pronounced in the cycles with higher deformation loading. Additionally, the hysteretic response of the specimen with 2X12 as shear reinforcement in the joint area was marginally lower, whereas the specimens of 2x16, which gave a better response, showed a marginally better response. Also, as compared the load difference it will be less than JA0 by 0.8%, 0.33%, 0.68%, and 0.71% for JC8, JC9, JC10, and JC11, respectively, and higher than JA1by 4.65%, 4.16%, 3.11%, and 3.08%.

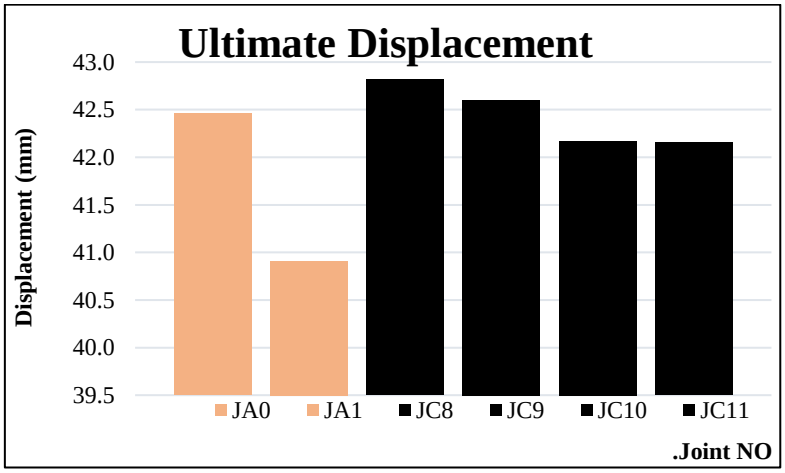

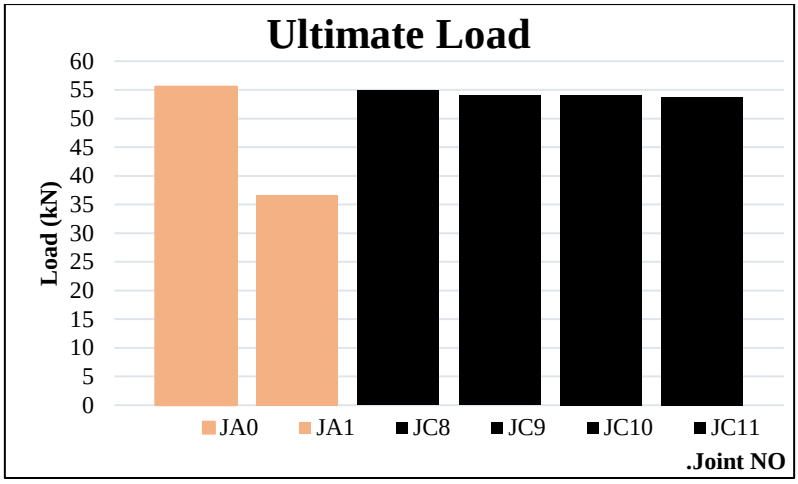

Figure 19: Result of group C compared with JA0 & JA1

As a result, the x-bar is improving the strength of the joint, but it is not adequate as compared with the ACI352R-02 recommendation for the same shear reinforcement ratio. Considering the cracking patterns, the absence of stirrups in the joint region combined with the deformations of the bend anchoring of the beam's bars (anchorage failure) resulted in considerable damage to the concrete cover behind the joint area. Stirrups kept the joint body noticeably undamaged by containing these deformations. Since a distinct flexural hinge evolved in the beam-joint interface, specimens with X-bars demonstrated increased damage mode performance.

3.2.4The effect of shear reinforcement for both joint and beam

This section studied two categories, the effect of stirrups' spacing of beam; and the ratio of shear reinforcement of joint core on the beam-column joint. From the hysteric response of group D that is illustrated in figure 20, the comparison will be at the same spacing of the beam's stirrups. As a result, at 65 spacing, the joint with reinforcement has a higher load carrying capacity than the joint without shear reinforcement, as shown in figures 20A & B. On the other hand, as compared to the JD12 & JD13 control specimens, this enhancement was reduced by 2% and 3%. The developed load carrying capacity could be more significant as changing the spacing of stirrups, as illustrated in figures 20C; D; E; F. When reducing the spacing to 50mm for specimen JD16 and JD17, the strength is enhanced by 30% and 27% respectively, as compared with specimen JB5. However, this developed disadvantage when comparing the JD16 and JD17 with JA0 by 1% and 3%, respectively. This spacing change the developer's strength more than ACI 318 recommends. However, according to the observations, column crossed inclined bars were a feasible option for improving the shear capacity of the cyclically loaded beam-column joints.

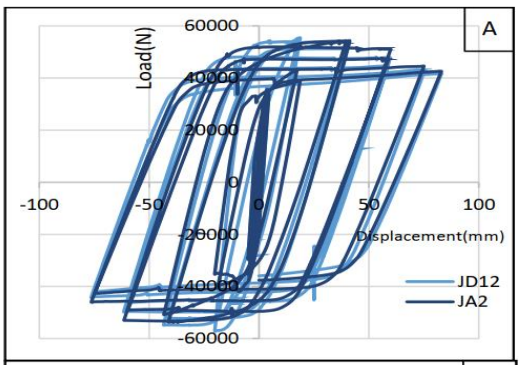

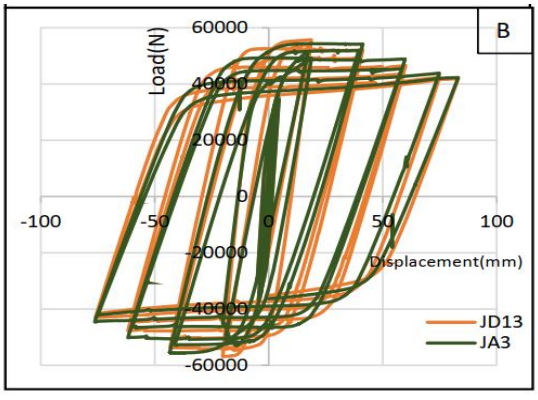

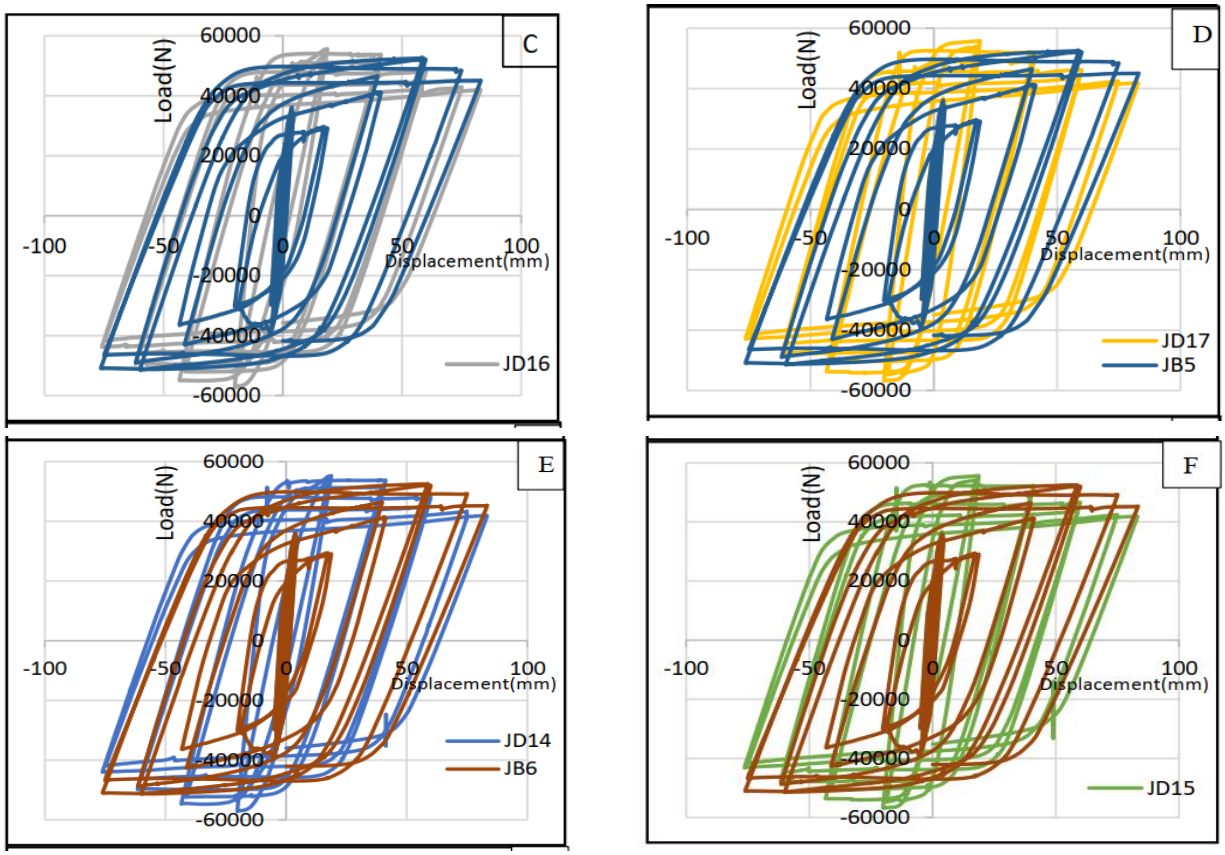

Figure 20. Comparison of hysteric response

The existence of inclined bars provides a new shear transmission mechanism. In addition, increasing the spacing to 70mm reduces the load carrying capacity to 3% and 4% for JD14 and JD15, respectively, when compared to JA0.Otherwise, it is developed by 28% and 26% with respect to JB6.

3.2.5 The influence of stirrups diameter of beam

For more investigation of the effect of shear reinforcement, four different stirrups diameter has been used in two groups one with ACI-designed joint (group E), whereas the other group F use 1.4 time of joint reinforcement of group E. the result for these groups is shown in Figure 21:

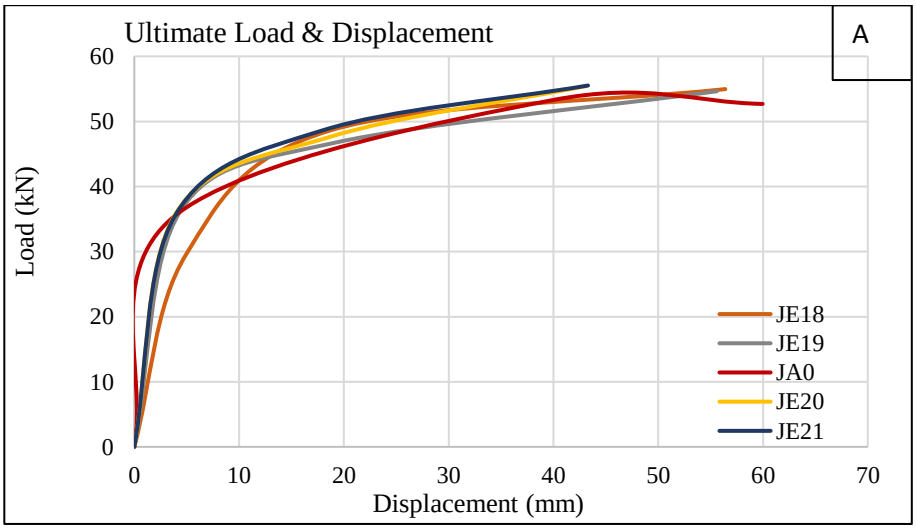

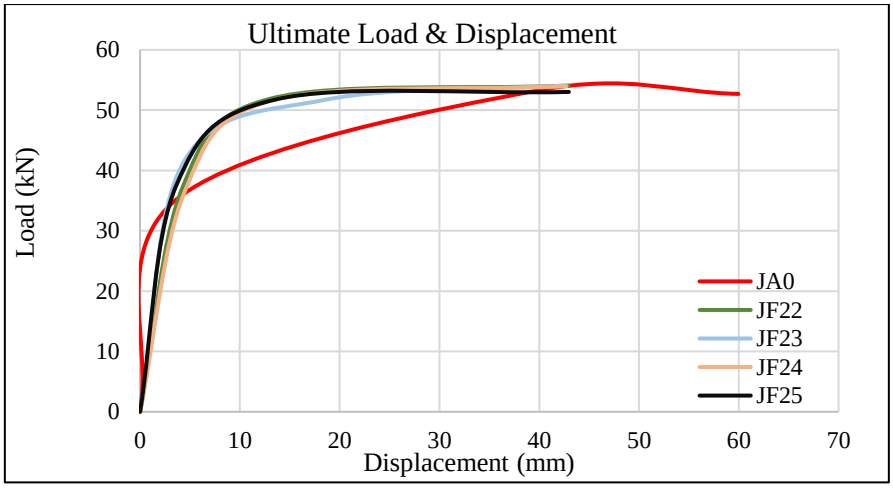

Figure 21. Envelope curve of ultimate load verse displacement; A) for group E and B) for group F

From the result of group E, the increase in the bar diameter causes the load capacity to increase by 1.44% and 0.04% for JE18 and JE19, respectively. The decrease in diameter leads to less strength by 0.20% and 0.23%. So, according to the previous percentage, the stirrup diameter has no significant effect on the load capacity of specimens as compared to JA0 at the ultimate load point. By increasing the diameter, the curve becomes more smooth, stronger and has a higher load capacity than that shown in figure 21 A. Furthermore, group F shows no significant change in both behaviour and skeleton and less difference respectively to JC9 as follows: when increasing the stirrup diameter, the load capacity increases by 0.13% and 0.42% for JF22 and JF23 respectively. In addition to decreasing the diameter, decreasing the load capacity by 0.08% and 1.82%, a 1% increase and decrease respectively. Therefore, there is no effective enhancement from this parameter as compared with JA0. All specimens have lower load bearing capacity by 2.66%, 2.38%, 2.87%, and 4.56% for JF22, JF23, JF24, and JF25, respectively. Because x-bar increases shear strength when used with joint ties, it is insufficient when used alone. All specimens were under severe shear failure for both beam and joint core. Increasing the diameter of the stirrups increases the risk of failure at the beam and vice versa.

3.2.6 The influence of flexural reinforcement

This section of group G illustrates the effect of flexural behavior on the beam-column joint by using three different diameters. The results are illustrated in Figure 22.

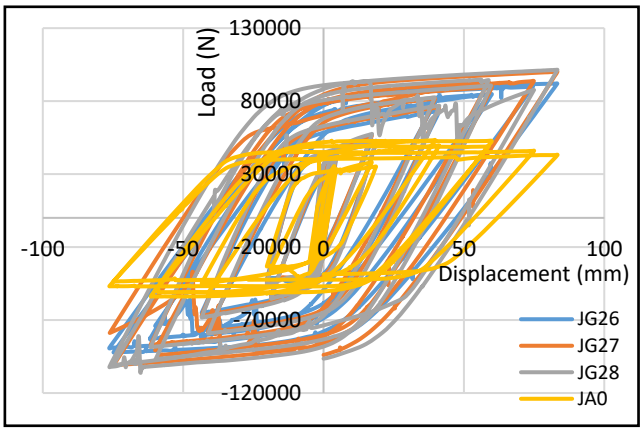

Figure 22. Hysteric response of group G and JA0 specimen

Increasing the reinforcement ratio leads to more strength and increases the load capacity of samples with respect to JA0 by 50%, 82%, and 84% for samples JG26, JG27, and JG28, respectively. From the hysteric response in figure22, the shape of JA0 is wider and shorter than other samples. As the bar diameter increases, the other samples have a higher load bearing capacity and are stiffer than JA0 (main reinforcement ratio).

3.2.7 Using horizontal x-bar (Type 2)

One of the most effective factors is plastic hinge of joint which the reason for cause the failure at interface, from the above sections the best parameter was increase the bar diameter. Although it prevents the failure at interface and enhance the load capacity but it made the joint core weaker so, at this part of study made the x-bar horizontal, that reduce the failure at joint as well as support the interface region. Anyway, to known the best distance of crossing bars explained at figure23, figure 23A explain that as goes toward the beam's tip it has lower effect whereas it has a significant effect at interface and at joint which is the better position for crossing the x-bars.

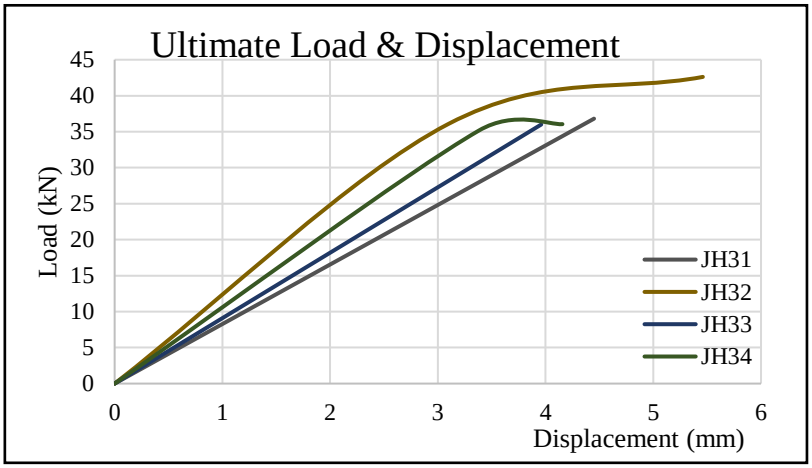

a)

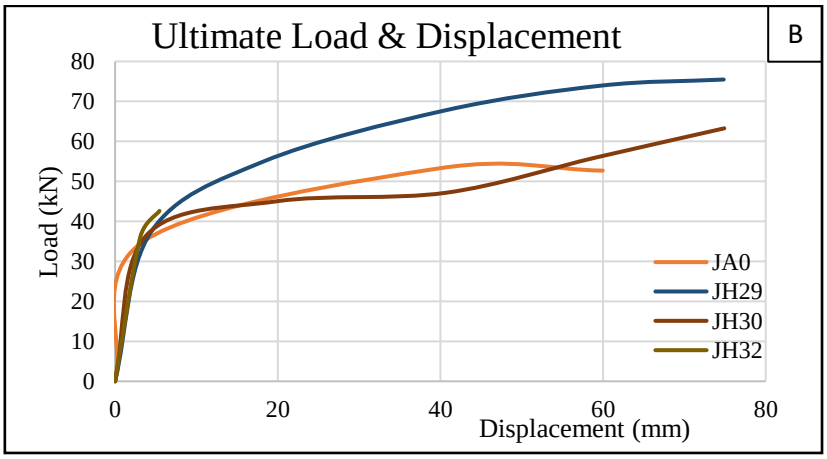

b)

Figure 23. A) The influence of x-bars at different position of beam; B) comparison between the control sample and group H

From the figure 24, the damage strain has the same value but not at the same position of damage region. The JH29 has the less damage at joint and the plastic hinge has an effect at the beam's middle region where the developmental length ended, otherwise all other cases the

plastic hinge effect was at the joint and interface in spite of the crossing of bars goes toward the beam's tip. If the values at the legend box are checked properly, they would be significantly more suitable than all other solutions except samples of group G.

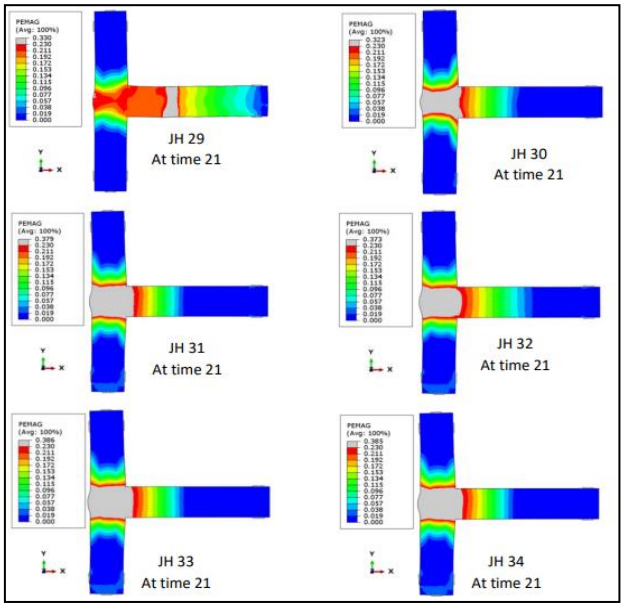

Figure 24. Plastic strain of group H

4. Conclusions

The conclusion of numerical result of beam-column joint under limited cycles of repeated loading could be drawn as following:

1. The validation result gives a good agreement with experiment as observed in load-displacement curve and a good difference for load capacity where the error was less than 8%.
2. The cracking was mostly localized at the beam-joint interface, creating a pronounced flexural hinge, in specimens with crossed inclined bars and stirrups. These specimens also displayed improved hysteretic response and excellent performance capabilities. The using of x-bars (Type1) at along the column enhances the joint as compared with non-shear reinforce joint but not significantly useful, except use high ratio. Otherwise use x-bar (Type2) along beam which give a good result at low ratio.
3. Using crossing bars type 2 in the centre region helps prevent damage to the joint core. Also, the use of a 1.2% reinforcement ratio of X-bar Type1 in addition to ties helps to prevent joint damage.
4. Using Type1 bars enhance the joint strength up to 250 kN (37%), by using Ø16, in contract with the Type2 bar that enhance the strength up to 37% by using Ø12, in addition to better behaviour of load-displacement curve as well as plastic strain damage.
5. Make the crossing bars point of Type 2 at different distances give a negative effect of load-displacement curve behaviour. The only case that gives a good behaviour at centre of joint behaviour.
6. Study the other parameter which are change of stirrups' spacing, stirrups diameter, increase the ratio of ties don't give a significant influence on the strength of the joint.
7. The increasing the flexural diameter (ratio of beam's bars) has a good influence on the load-displacement curve as well as improved the behaviour of the plastic strain. Therefore, the best ratio of the beam's flexural ratio is about 0.4%. Using more than this percentage will be excessive steel reinforcement.

References

[1] C. Karayannis, and G. Sirkelis, "Effectiveness of RC beam-column connections strengthening using carbon-FRP jackets," Earthquake Engineering and Structural Dynamics, vol.37, pp. 769-790, April 2008.

[2] M. Favvata, B. Izzuddin, and C. Karayannis, "Modelling exterior beam-column joints for seismic analysis of RC frame structures, " Earthquake Engineering and Structural Dynamics, vol. 37, pp. 1527–1548, July 2008.

[3] T. Saito, and M. Kikuchi, "A new analytical model for reinforced concrete beam-column joints subjected to cyclic loading, " In Proceedings Of The Fifthteenth World Conference On Earthquake Engineering Lisbon, Portugal, Vol.2012, September 2012.

[4] Vecchio, F.J. and Collins, M.P. ″The Modified Compression-Field Theory for Reinforced Concrete Elements Subjected to Shear″. American Concrete Institute Journal., Vol. 83, NO.2, pp.219-231, 1986.

[5] G. Diro, and W. Kabeta, "Finite element analysis of key influence parameters in reinforced concrete exterior beam column connection subjected to lateral loading, " European Journal of Engineering Research and Science, vol. 5, pp.689-697, June 2020.

[6] Cao, Y., Wakil, K., Alyousef, R., Jermsittiparsert, K., Ho, L. S., Alabduljabbar, H., ... & Mohamed, A. M, ″Application of extreme learning machine in behavior of beam to column connections″. In Structures Journal, Vol. 25, pp. 861-867, June, 2020.

[7] Al-Jumaily, G. A., & Rahman, A. A. A. ″Simulation of reinforced concrete beam-column joints under cyclic loading″. In *Journal of Physics: Conference Series*, Vol. 1895, No. 1, p. 012052. IOP Publishing, May 2021.

[8] C. Chalioris, C. Karayannis, and M. Favvata, "Cyclic testing of reinforced concrete beam-column joints with crossed inclined bars, " WIT Transactions on Modelling and Simulation, vol. 46, pp.623-632, May 2007.

[9] L. Saenz, "Discussion of equation for the stress-strain curve of concrete-by Desayi, P. and Krishan, S." Journal of American Concrete Institute, vol. 61, pp. 1229–1235,1964.

[10] P.S. Wang, and F.J. Vecchio, "VecTor2 and formworks user manual, " University of Toronto, Canada, 2006.

[11] A. Genikomsou, and M.Polak, "Finite element analysis of punching shear of concrete slabs using damaged plasticity model in ABAQUS," Engineering Structures, vol. 98, pp. 38–48, April 2015.

[12] Sahoo, P., Chatterjee, B., & Adhikary, D. ″Finite Element Based Elastic-Plastic Contact Behavior of a Sphere Against A Rigid Flat-Effect Of Strain Hardening″. International Journal of Engineering and Technology, Vol. 2, NO.1, pp.1-6,2010.

[13] Dunne, F., & Petrinic, N. ″Introduction to Computational Plasticity″. Oxford University Press, 2005.

[14] A. Belarbi, and T. Hsu, "Constitutive laws of concrete in tension and reinforcing bars stiffened by concrete," Structural Journal of the American Concrete Institute, vol. 91, pp.465-474, 1994.

[15] J. Sebastian, and V. Philip, "An analytical investigation on improving ductile reinforcement of exterior beam column joints, " International Journal of Innovative Research in Technology, vol.3, pp.138-147, September 2016.

[16] ABAQUS Analysis user's manual 6.16-EF (2016). Dassault Systems Simulia Corp. Providence, RI, USA.

[17] ACI 318-19. (2019). Building Code Requirements for Structural Concrete, Reported by American Concrete Institute Committee 318.

[18] P. Bakir, "Seismic resistance and mechanical behaviour of exterior beam - column joints with crossed inclined bars," Journal of Structural Engineering and Mechanics, vol.16, pp. 493-517, 2003.

[19] ACI Committee 318. Building code requirements for structural concrete (ACI 318-02) and commentary (ACI 318R-02). American Concrete Institute, Farmington Hills, Mich., 2002.

[20] ACI-ASCE Committee 352. Recommendations for design of beam-column connections in monolithic reinforced concrete structures (ACI 352R-02). American Concrete Institute, Farmington Hills, Mich., 2002.